

Article

# Limonin, a Component of *Dictamni Radicis Cortex*, Inhibits Eugenol-Induced Calcium and cAMP Levels and PKA/CREB Signaling Pathway in Non-Neuronal 3T3-L1 Cells

Yeo Cho Yoon <sup>1,†</sup>, Sung-Hee Kim <sup>1,†</sup>, Min Jung Kim <sup>1</sup>, Hye Jeong Yang <sup>1</sup>, Mee-Ra Rhyu <sup>1</sup>  
and Jae-Ho Park <sup>1,2,\*</sup>

Received: 16 October 2015 ; Accepted: 2 December 2015 ; Published: 10 December 2015

Academic Editor: Derek J. McPhee

<sup>1</sup> Division of Functional Food Research, Korea Food Research Institute, 1201-62 Anyangpangyo-ro, Bundang-gu, Seongnam-si, Gyeonggi-do 463-746, Korea; Yoon.Yeo-cho@kfri.re.kr (Y.C.Y.); Kim.Sung-hee@kfri.re.kr (S.-H.K.); kmj@kfri.re.kr (M.J.K.); yhj@kfri.re.kr (H.J.Y.); mrrhyu@kfri.re.kr (M.-R.R.)

<sup>2</sup> Food Biotechnology, University of Science & Technology, 217 Gajeong-ro, Yuseong-gu, Daejeon 305-350, Korea

\* Correspondence: jaehopark@kfri.re.kr; Tel.: +82-31-780-9337; Fax: +82-31-780-9360

† These authors contributed equally to this work.

**Abstract:** Limonin, one of the major components in *dictamni radicis cortex* (DRC), has been shown to play various biological roles in cancer, inflammation, and obesity in many different cell types and tissues. Recently, the odorant-induced signal transduction pathway (OST) has gained attention not only because of its function in the perception of smell but also because of its numerous physiological functions in non-neuronal cells. However, little is known about the effects of limonin and DRC on the OST pathway in non-neuronal cells. We investigated odorant-stimulated increases in  $Ca^{2+}$  and cAMP, major second messengers in the OST pathway, in non-neuronal 3T3-L1 cells pretreated with limonin and ethanol extracts of DRC. Limonin and the extracts significantly decreased eugenol-induced  $Ca^{2+}$  and cAMP levels and upregulated phosphorylation of CREB and PKA. Our results demonstrated that limonin and DRC extract inhibit the OST pathway in non-neuronal cells by modulating  $Ca^{2+}$  and cAMP levels and phosphorylation of CREB.

**Keywords:** limonin; furanolactone; cAMP; olfactory; calcium; *dictamni radices cortex*

## 1. Introduction

*Dictamni radicis cortex* (DRC), a root of *Dictamnus dasycarpus* Turcz, is native to East Asia and has been used as a traditional Korean medicine to treat various diseases, such as allergic dermatitis, jaundice, hepatitis, and rheumatism [1,2]. Using molecular analysis, Sun *et al.* demonstrated the anti-platelet aggregation activity of DRC [3]. Limonin (Figure 1) was first isolated from citrus [4] and is a known component of DRC [5], and many studies have demonstrated its efficacy in the treatment of cancer, inflammation, and obesity [6–8]. Limonin affects the expression of lipid metabolism-related genes in 3T3-L1 cells, an *in vitro* model system for the study of adipogenesis [9]. In addition, 3T3-L1 cells are widely used to examine many biological phenomena, such as glucose uptake, apoptosis, and cell cycle [10–12]. Yoon *et al.* first demonstrated the utility of 3T3-L1 cells as a model system to study odorant-induced signal transduction (OST) pathway in non-neuronal cells by showing that an olfactory receptor involved in the OST pathway is expressed in 3T3-L1 cells and the OST pathway can be regulated by an exogenous molecule [13].

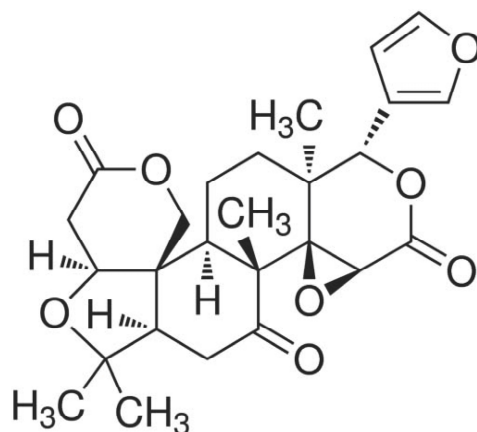


**Figure 1.** Structure of limonin used in this study.

The olfactory system is necessary for survival, since it is intricately involved in mating, avoidance of predators, fear, and food selection. Olfactory receptors are mainly localized to the cilia on the olfactory sensory neurons (OSN) [14]. The binding of odorants to their receptors is the first step for the perception of smell. The activated receptors increase intracellular cAMP and  $\text{Ca}^{2+}$  levels, which lead to depolarization of the membrane potential. This signal is transmitted to the brain and is perceived as smell [15,16]. There is emerging evidence demonstrating that ORs ectopically expressed in non-neuronal tissues [17] may have distinct physiological functions [18–23]. Importantly, the crucial signaling cascade of cAMP and  $\text{Ca}^{2+}$  is conserved across neuronal and non-neuronal tissues [19–22].

In this study, we investigated whether DRC affects the OST pathway in non-neuronal 3T3-L1 cells and determined the amount of limonin in DRC. The effects of limonin on the OST pathway were also examined.

## 2. Results and Discussion

### 2.1. DRC Decreased $\text{Ca}^{2+}$ and cAMP Levels in 3T3-L1 Cells

Previously, we reported that stimulation with eugenol increased  $\text{Ca}^{2+}$  and cAMP levels in non-neuronal 3T3-L1 cells [13]. Here, we investigated the effect of ethanol extracts of DRC on the eugenol-induced signaling pathway. In Figure 2A,  $\text{Ca}^{2+}$  levels dramatically decreased in response to 100–800  $\mu\text{g}/\text{mL}$  of DRC extracts while DRC alone without eugenol did not affect calcium level. Since cAMP levels are known to modulate  $\text{Ca}^{2+}$  levels in the OST pathway [15], we examined the effect of DRC extract on cAMP levels in 3T3-L1 cells. As shown in Figure 2B, eugenol-induced cAMP levels decreased after treatment with 200–800  $\mu\text{g}/\text{mL}$  of DRC extracts. In addition, DRC alone did not affect cAMP level. Together with calcium without eugenol, it demonstrated that DRC specifically inhibits eugenol-induced calcium and cAMP increases. Although 100  $\mu\text{g}/\text{mL}$  of extracts did not significantly decrease cAMP level (data not shown), it decreased the calcium level. This variation may be owing to differential conditions of the assay systems, including stimulation time, sensitivity of the systems, and temperature at which cAMP and calcium levels were measured. Importantly, 200–800  $\mu\text{g}/\text{mL}$  extracts of DRC reduced both measures,  $\text{Ca}^{2+}$  and cAMP, of OST pathway activation, suggesting that the DRC extracts inhibited the OST pathway in eugenol-induced 3T3-L1 cells. To determine whether these inhibitory effects were due to the toxicity of the extracts, we examined cell viability with extract treatment. As shown in Figure 2C, pretreatment with the extracts (100–800  $\mu\text{g}/\text{mL}$ ) for 30 min did not affect the proliferation of 3T3-L1 cells, demonstrating that inhibition of  $\text{Ca}^{2+}$  and cAMP levels by these extracts was not caused by cell toxicity.

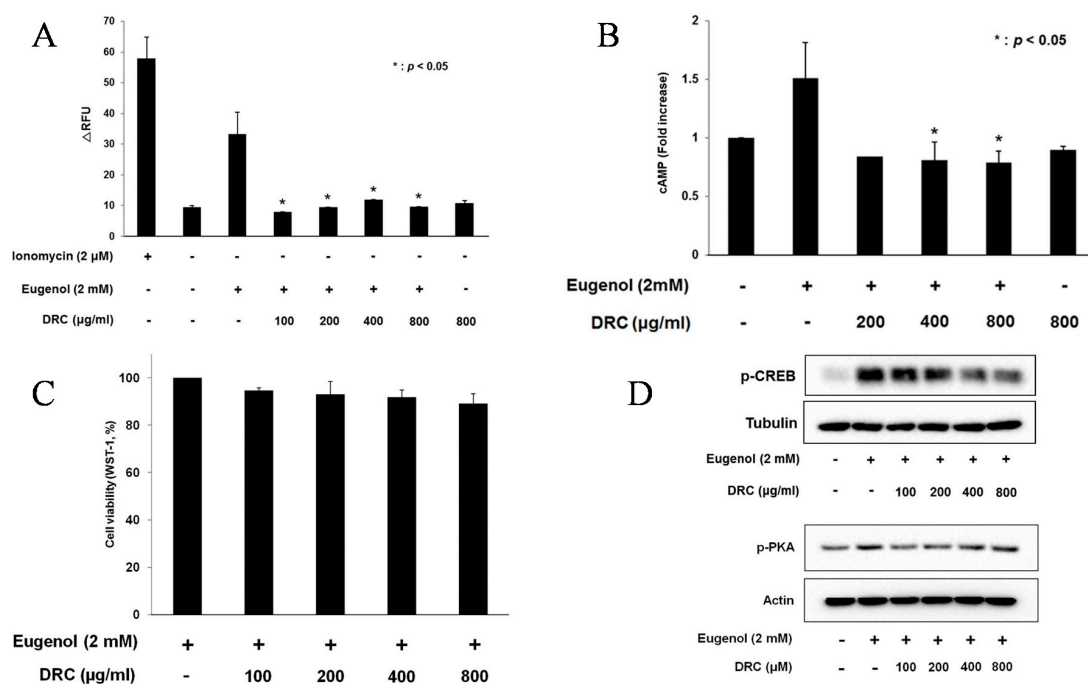


**Figure 2.** (A) The ethanol extracts of dictamni radices cortex (DRC) decreased Ca<sup>2+</sup> levels in eugenol-induced 3T3-L1 cells. Ionomycin (2 μM) and DMSO (0.2%) were used as positive and negative controls, respectively. Cells were treated with DRC extracts for 30 min, and Ca<sup>2+</sup> levels were measured after stimulation with eugenol (2 mM). The data are shown as means ± SD (*n* = 3). \*: *p* < 0.05, ΔRFU: change in relative fluorescence unit; (B) Changes in cAMP level after pretreatment with the ethanol extracts of dictamni radices cortex (DRC) for 30 min. The high concentration of DMSO was 0.2% in this experiment. The data are shown as means ± SD (*n* = 3). \*: *p* < 0.05; (C) Cell viability. 3T3-L1 cells were treated with dictamni radices cortex (DRC) extracts for 30 min. Cell proliferation was evaluated by WST-8 assay. The data are shown as means ± SD (*n* = 3); (D) Phosphorylated protein kinase A (PKA) and cAMP response element binding protein (CREB) protein levels by Western blot in the 3T3-L1 cells after pretreatment with the ethanol extracts of dictamni radices cortex (DRC) for 30 min. A total of 35 μg of protein was separated by sodium dodecyl sulfate polyacrylamide gel electrophoresis (SDS-PAGE).

## 2.2. DRC Decreased the Phosphorylation of CREB in 3T3-L1 Cells

To investigate the effects of DRC on the OST pathway, phosphorylation of PKA and CREB, known downstream targets of cAMP [23], was carefully examined. As shown in Figure 2D, treatment with DRC extracts (200–800 μg/mL) decreased the phosphorylation of CREB, whereas the phosphorylation of PKA decreased at lower concentration (100–200 μg/mL) and increased at higher concentrations (400 and 800 μg/mL). Although it remains unclear, it is possible that additional components of the ethanol extracts including choline, its derivatives, sitosterol, and campesterol of DRC may differentially affect phosphorylation of these target proteins, which is supported by a report demonstrating that a choline's derivative can stimulate PKA [24].

## 2.3. Determination of Limonin in the Ethanol Extract of DRC Using UPLC-MS/MS

Next, we measured the amount of limonin in the DRC extracts using UPLC-MS/MS. As shown in Figure 3A, the retention time of limonin was 3.7 min, and its molecular mass was 470.52 Da. The mass peak was characterized using a mass spectrometer. The parent-to-daughter ion transitions were monitored at *m/z* 471.3 → 161.3 (Figure 3B). To determine the concentration of limonin in the extracts, the external calibration curve was first generated with the external limonin. The fitted curve with linear regression was  $Y = 37.812X + 870.5$  with an *R*<sup>2</sup> value of 0.981. The limonin content

was calculated with the peak area and the calibration curve. The concentration of limonin was  $0.216 \pm 0.0007$  mg/100 g of the ethanol extracts.

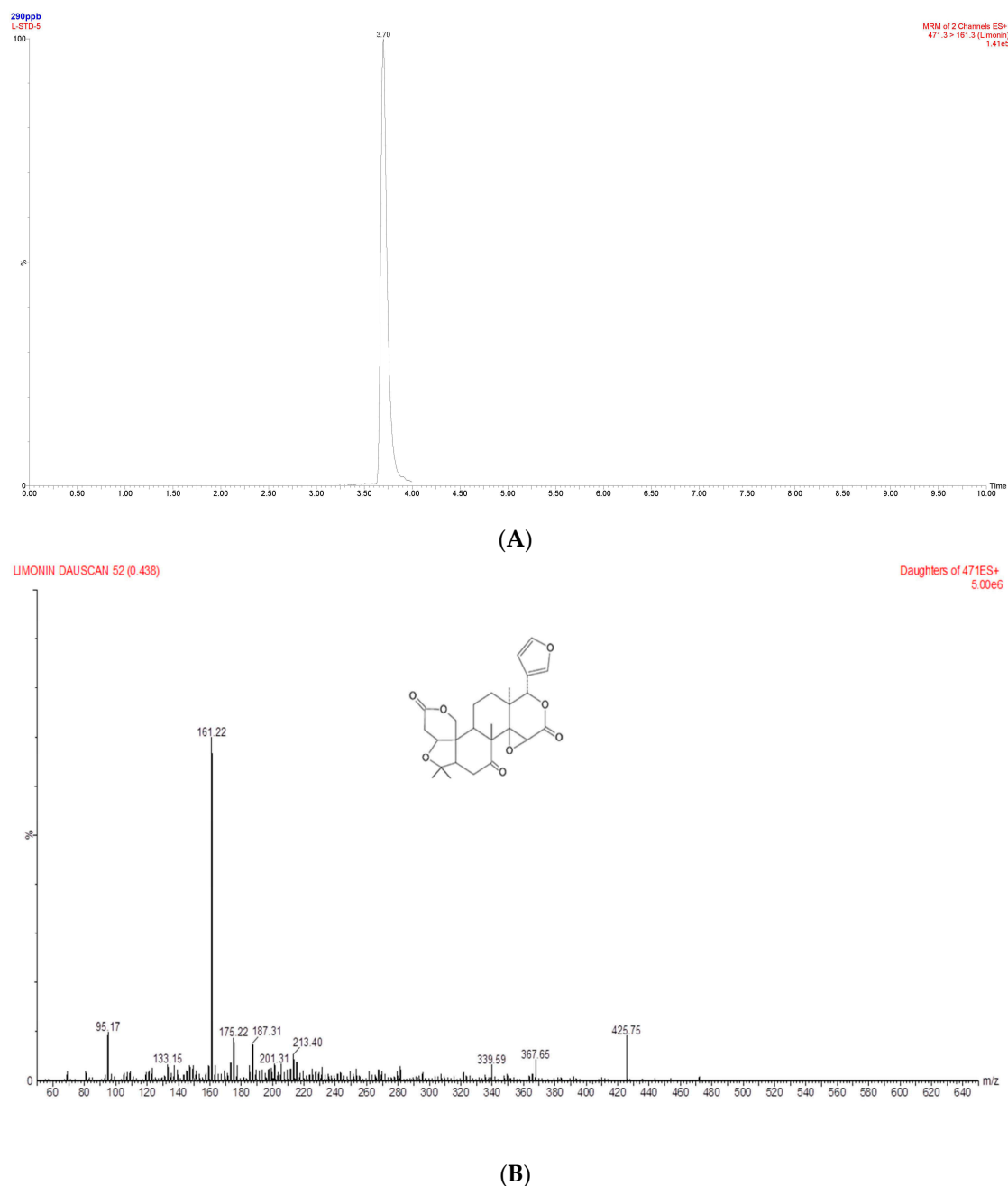


**Figure 3.** (A) Representative UPLC-MS/MS chromatograms of limonin; (B) Full-scan product ion spectra of  $[M + H]^+$  ions and fragmentation pathways for limonin.

#### 2.4. Limonin Suppressed Eugenol-Induced $Ca^{2+}$ and cAMP: Levels in 3T3-L1 Cells

In Section 3.3, we showed that limonin is one of the components of DRC extracts; therefore, we investigated the effects of limonin on the OST pathway in 3T3-L1 cells. After pretreatment with limonin, calcium levels were measured under the same conditions as previously described for DRC extracts. As shown in Figure 4A, eugenol-induced  $Ca^{2+}$  levels were dose dependently decreased with 200–1600  $\mu$ M limonin. However, limonin alone did not affect calcium level. Similarly, cAMP levels were decreased by up to 40% after pretreatment with 400–1600  $\mu$ M limonin compared to the

positive control (Figure 4B), while limonin did not affect cAMP level. These strongly suggest that limonin, at least, specifically inhibits eugenol-induced calcium and cAMP level in 3T3-L1 cells. However, it could not be excluded the possibility that limonin affects other signaling pathways in the cells. To determine toxicity by limonin, cell viability was assessed in cells treated with limonin. As shown in Figure 4C, up to 1.6 mM limonin did not affect cell viability. These results suggest that limonin inhibits  $\text{Ca}^{2+}$  and cAMP levels in eugenol-induced 3T3-L1 cells.

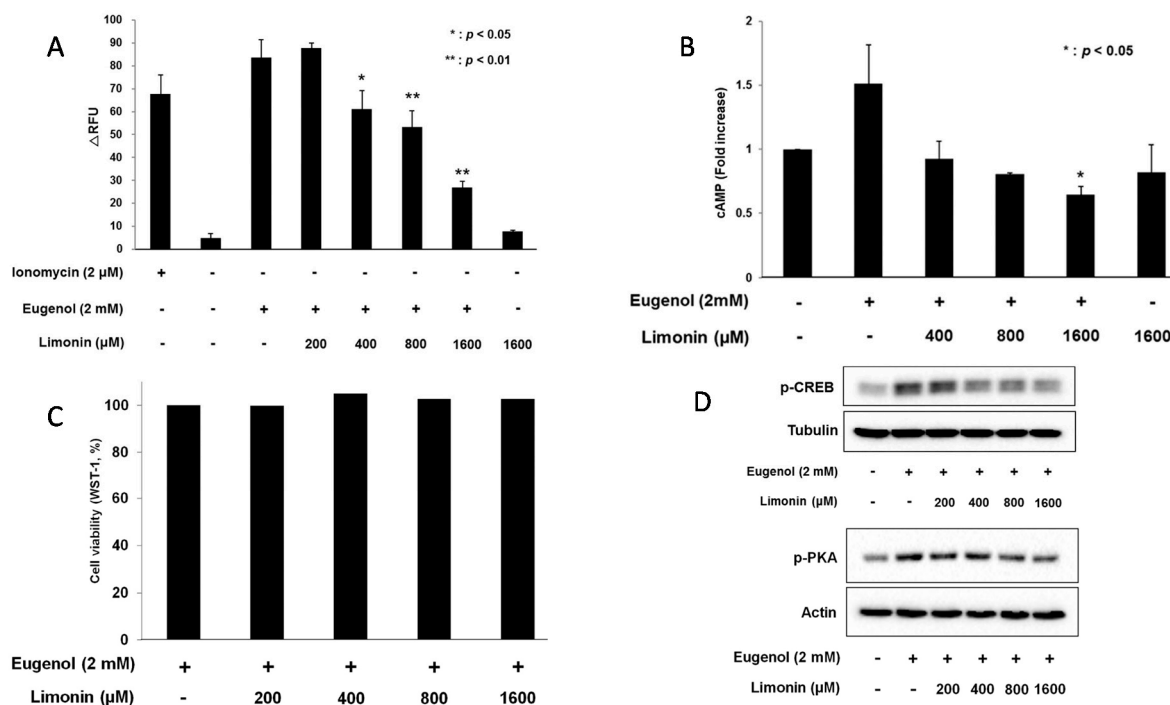


**Figure 4.** (A) Changes of  $\text{Ca}^{2+}$  levels with limonin pretreatment in eugenol-induced 3T3-L1 cells. Ionomycin (2 μM) and DMSO (0.2%) were used as positive and negative controls, respectively. The data are shown as means  $\pm$  SD ( $n = 3$ ). \*:  $p < 0.05$ , \*\*:  $p < 0.01$ , ΔRFU: change in relative fluorescence unit; (B) Pretreatment with limonin for 30 min changes cAMP levels in eugenol-induced 3T3-L1 cells. The final concentration of DMSO was 0.2%. The data represent means  $\pm$  SD ( $n = 3$ ). \*:  $p < 0.05$ ; (C) Cell viability. 3T3-L1 cells were treated with limonin for 30 min. Cell proliferation was evaluated by WST-8 assay. The data are shown as means  $\pm$  SD ( $n = 3$ ); (D) Phosphorylated protein kinase A (PKA) and cAMP response element binding protein (CREB) levels in 3T3-L1 cells after pretreatment with limonin for 30 min. A total of 35 μg of protein was separated by SDS-PAGE. In experiments for Western blot analysis, the final concentration of DMSO was 0.2%.

### 2.5. Limonin Decreased Eugenol-Induced Phosphorylation of PKA and CREB in 3T3-L1 Cells

In order to elucidate the effects of limonin on the OST pathway in non-neuronal cells, we examined the levels of eugenol-induced phosphorylation of PKA and CREB in limonin-pretreated cells. As shown in Figure 4D, the phosphorylation of PKA and CREB was significantly decreased by limonin in dose-dependent manner. These data suggest that limonin inhibits eugenol-induced phosphorylation of CREB and PKA in non-neuronal 3T3-L1 cells.

### 3. Experimental Section

#### 3.1. Plant Material

Ethanol extract of DRC was obtained from the Korea plant extract bank at the Korea Research Institute of Bioscience and Biotechnology (KRIBB, Daejeon, Korea). The powder was dried at room temperature and then dissolved in dimethylsulfoxide (DMSO) (*v/v*).

#### 3.2. Reagents and Antibodies

Eugenol and limonin were purchased from Sigma (St. Louis, MO, USA). The  $\text{Ca}^{2+}$  assay kit was obtained from Molecular Devices (Sunnyvale, CA, USA), and the cAMP assay kit was purchased from Enzo Life Sciences, Inc. (Farmington, NY, USA). Antibodies against phospho-protein kinase A (PKA) and phospho-cyclic AMP response element binding protein (CREB) were purchased from Cell Signaling Technology (Beverly, MA, USA), and the actin antibody was obtained from Bethyl Laboratories (Montgomery, TX, USA).

#### 3.3. Cell Culture

3T3-L1 cells were purchased from American Type Culture Collection (Manassas, VA, USA) and cultured in Dulbecco's Modified Eagle Medium (DMEM) (high glucose), which contained 10% fetal bovine serum (FBS) and  $1\times$  antibiotic-antimycotic solution (Welgene Inc., Daegu, Korea). The cells were incubated at 37 °C in the presence of 5%  $\text{CO}_2$ .

#### 3.4. $\text{Ca}^{2+}$ Assay

The 3T3-L1 cells were seeded in 96-well black plates and pretreated with DRC and limonin in a  $\text{CO}_2$  incubator for 30 min. Then, 100  $\mu\text{L}$  component A buffer (Molecular Devices) was added, and the plate was covered with foil and incubated for 30 min at room temperature and then 15 min at 37 °C. Eugenol and ionomycin were automatically added in Flexstation 3 (Molecular Devices), and the  $\text{Ca}^{2+}$  level was measured according to the manufacturer's instructions.

#### 3.5. cAMP Assay

3T3-L1 cells were starved with serum-free DMEM (high glucose) media for 16–18 h, and cells were pretreated with DRC and limonin for 30 min. Cells were then treated with eugenol for 7 min and lysed with 0.1 M HCl. cAMP levels were measured using the Direct cAMP ELISA kit (Enzo Life Sciences).

#### 3.6. Cell Viability Analysis

The viability of cells was determined using the Cell Counting Kit-8 Reagent (CCK-8) (Enzo Life Sciences). Cells at a concentration of  $5 \times 10^4$  cells/well in 200  $\mu\text{L}$  culture medium were seeded in a 96-well plate. The cells were incubated for 8 h at 37 °C and 5%  $\text{CO}_2$  and starved for 16 h with serum-free medium, and then treated with DRC or limonin in 200  $\mu\text{L}$  serum-free medium. After incubating cells with 10  $\mu\text{L}$ /well CCK-8 reagent for 4 h, the absorbance of the samples was measured using a microplate reader at 450 nm.

#### 3.7. Western Blot Analysis

Cells were seeded in 6-well plates and starved with serum-free DMEM for 16–18 h. The starved cells were pretreated with DRC and limonin for 30 min and treated with eugenol for 7 min. The cells were lysed with RIPA buffer (Bioseang, Seongnam-si, Korea), which contained a protease inhibitor cocktail (Roche, Basel, Switzerland) and a phosphatase inhibitor cocktail (Roche). The lysate was centrifuged at 12,000 rpm for 30 min at 4 °C. Protein concentration was measured using the SMART bicinchoninic assay (BCA) Protein Assay Kit (Intron Biotechnology, Seongnam-si, Korea). A total

of 35 µg of the protein was separated on a 10% SDS-PAGE and transferred onto a nitrocellulose membrane. The membranes were blocked with 5% skim milk in 1 × Tris-buffered saline (TBS) containing Tween 20 (TBST) for 1 h at room temperature and incubated with primary antibodies at 4 °C for 16–18 h. The membranes were probed with horseradish peroxidase (HRP)-conjugated secondary antibody at room temperature for 1 h, and then immuno-reactive bands were visualized using enhanced chemiluminescence reagents (Amersham, Piscataway, NJ, USA).

### 3.8. Ultra-Performance Liquid Chromatography Tandem Mass Spectrometry (UPLC–MS/MS) Analysis

The analyses were performed using an Acquity UPLC system (Waters, Miliford, MA, USA) with Acquity UPLC BEH C18 column (2.1 mm × 100 mm, 1.7 µm). The mobile phase included 0.1% formic acid aqueous solution (Solvent A) and 0.1% formic acid in acetonitrile (Solvent B), and a gradient elution program was performed: 90% solvent A (0 min)-50% solvent A (3 min)-90% solvent A (5 min), at a flow rate of 0.3 mL/min. Column temperature was kept at 40 °C and the total run time was 5 min. The auto-sampler was conditioned at 4 °C and the injection volume was 5 µL. Identification and quantification of limonin for AP was carried out on a Waters Xevo TQ triple-quadrupole mass spectrometer equipped with electro spray ionization (ESI) mode. The ESI source was set in positive ESI mode and processed using MassLynx 4.1 (Waters) software. The quantification was performed using multiple reaction monitoring (MRM) mode of  $m/z$  471.3 → 161.3 for limonin. The detector was operated in cone voltage 32 V, a capillary voltage 3.3 kV. The source temperature was set at 150 °C while the desolvation flow was set at 800 L/h; the desolvation gas temperature was set at 400 °C

### 3.9. Statistical Analysis

All experiments were repeated at least three times, and the data are expressed as the mean ± standard deviation (SD). Group means were compared using the non-parametric Kruskal-Wallis and Mann-Whitney analysis using SPSS (SPSS Inc., Armonk, NY, USA).

## 4. Conclusions

In summary, our study, for the first time, demonstrated that ethanol extracts of DRC and limonin inhibit the OST pathway by regulating  $Ca^{2+}$  influx, cAMP levels, and phosphorylation of CREB in non-neuronal 3T3-L1 cells. These results expand our understanding of OST pathway in non-neuronal cells and provide non-neuronal cell system to investigate novel functions of olfactory receptor(s) and its regulation by exogenous molecules such as DRC and limonin. Our study also provides an *in vitro* cell system to characterize intrinsic ligands stimulating eugenol receptor which may has physiological functions in 3T3-L1 cells.

**Acknowledgments:** This study was supported by a grant from the Korea Food Research Institute (E00111202-05).

**Author Contributions:** Y.C.Y., S.H.K., M.J.K., and H.J.Y. performed the experiments and analyzed the data. Y.C.Y., S.H.K., and M.J.K. contributed drafting the manuscript. H.J.Y., M.R.R., and J.H.P. designed the experiments. J.H.P. wrote the paper.

**Conflicts of Interest:** The authors declare no conflict of interest.

## References

1. Jiang, S.; Nakano, Y.; Rahman, M.A.; Yatsuzuka, R.; Kamei, C. Effects of a *Dictamnus dasycarpus* T. Extract on Allergic Models in Mice. *Biosci. Biotechnol. Biochem.* **2008**, *72*, 660–665. [[CrossRef](#)] [[PubMed](#)]
2. Lv, M.; Xu, P.; Tian, Y.; Liang, J.; Gao, Y.; Xu, F.; Zhang, Z.; Sung, J. Medicinal uses, phytochemistry and pharmacology of the genus *Dictamnus* (Rutaceae). *J. Ethnopharmacol.* **2015**, *171*, 247–263. [[CrossRef](#)] [[PubMed](#)]
3. Sun, J.B.; Qu, W.; Wang, P.; Wu, F.H.; Wang, L.Y.; Liang, J.Y. Degraded limonoids and quinoline alkaloids from *Dictamnus angustifolius* G. Don ex Sweet and their anti-platelet aggregation activity. *Fitoterapia* **2013**, *90*, 209–213. [[CrossRef](#)] [[PubMed](#)]

4. Geissman, T.A.; Tulagin, V. Some observations on the structure of limonin. *J. Org. Chem.* **1946**, *11*, 760–770.
5. Du, C.F.; Yang, X.X.; Tu, P.F. Studies on chemical constituents in bark of dictamnus dasycarpus. *Zhongguo Zhong Yao Za Zhi* **1992**, *30*, 1663–1666.
6. Shimizu, S.; Miyamoto, S.; Fujii, G.; Nakanishi, R.; Onuma, W.; Ozaki, Y.; Fujimoto, K.; Yano, T.; Mutoh, M. Suppression of intestinal carcinogenesis in *Apc*-mutant mice by limonin. *J. Clin. Biochem. Nutr.* **2015**, *57*, 39–43. [[CrossRef](#)] [[PubMed](#)]
7. Kim, W.; Fan, Y.Y.; Smith, R.; Patil, B.; Jayaprakasha, G.K.; McMurray, D.N.; Chapkin, R.S. Dietary curcumin and limonin suppress CD<sup>4+</sup> T-cell proliferation and interleukin-2 production in mice. *J. Nutr.* **2009**, *139*, 1042–1048. [[CrossRef](#)] [[PubMed](#)]
8. Ono, E.; Inoue, J.; Hashidume, T.; Shimizu, M.; Sato, R. Anti-obesity and anti-hyperglycemic effects of the dietary citrus limonoid nomilin in mice fed a high-fat diet. *Biochem. Biophys. Res. Commun.* **2011**, *410*, 677–681. [[CrossRef](#)] [[PubMed](#)]
9. Halder, D.; Das, N.D.; Jung, K.H.; Choi, M.R.; Kim, M.S.; Lee, S.R.; Chai, Y.G. Cyclodextrin-clathrated limonin suppresses diet-induced obesity in mice. *J. Food Biochem.* **2014**, *38*, 216–226. [[CrossRef](#)]
10. Nugent, C.; Prings, J.B.; Whitehead, J.P.; Savage, D.; Wentworth, J.M.; Chatterjee, V.K.; O’Rahilly, S. Potentiation of glucose uptake in 3T3-L1 adipocytes by PPAR gamma agonists in maintained in cells expressing a PPAR gamma dominant-negative mutant: Evidence for selectivity in the downstream responses to PPAR gamma activation. *Mol. Endocrinol* **2001**, *15*, 1729–1738. [[PubMed](#)]
11. Rayalam, S.; Yang, J.Y.; Ambati, S.; Della-Fera, M.A.; Baile, C.A. Resveratrol induces apoptosis and inhibits adipogenesis in 3T3-L1 adipocytes. *Phytother. Res.* **2008**, *22*, 1367–1371. [[CrossRef](#)] [[PubMed](#)]
12. Reichert, M.; Eick, D. Analysis of cell cycle arrest in adipocyte differentiation. *Oncogene* **1999**, *18*, 459–466. [[CrossRef](#)] [[PubMed](#)]
13. Yoon, Y.C.; Kim, S.H.; Hwang, J.T.; Sung, M.J.; Kim, M.S.; Hur, H.J.; Rhyu, M.R.; Park, J.H. Ethanol extract of Polygonatum officinale rhizome inhibits odorant-induced cAMP and calcium levels in non-chemosensory 3T3-L1 cells. *J. Food Nutr. Res.* **2014**, *2*, 776–780. [[CrossRef](#)]
14. Buck, L.; Axel, R. A novel multigene family may encode odorant receptors: a molecular basis for odor recognition. *Cell* **1991**, *65*, 175–187. [[CrossRef](#)]
15. Restrepo, D.; Teeter, J.H.; Schild, D. Second messenger signaling in olfactory transduction. *J. Neurobiol.* **1996**, *20*, 37–48. [[CrossRef](#)]
16. Sakano, H. Neural map formation in the mouse olfactory system. *Neuron* **2010**, *67*, 530–542. [[CrossRef](#)] [[PubMed](#)]
17. Kang, N.; Koo, J. Olfactory receptors in non-chemosensory tissues. *BMB Rep.* **2012**, *45*, 612–622. [[CrossRef](#)] [[PubMed](#)]
18. Spehr, M.; Gisselmann, G.; Poplawski, A.; Riffell, J.A.; Wetzell, C.H.; Zimmer, R.K.; Haat, H. Identification of a testicular odorant receptor mediating human sperm chemotaxis. *Science* **2003**, *299*, 2054–2058. [[CrossRef](#)] [[PubMed](#)]
19. Fukuda, N.; Yomogida, K.; Okabe, M.; Touhara, K. Functional characterization of a mouse testicular olfactory receptor and its role in chemosensing and in regulation of sperm motility. *J. Cell Sci.* **2004**, *117*, 5835–5845.
20. Pluznick, J.L.; Zou, D.; Zhang, X.; Yan, Q.; Rodriguez-Gil, D.; Eisner, C.; Wells, E.; Greer, C.A.; Wang, T.; Firestein, S.; Schnermann, J.; Caplan, M.J. Functional expression of the olfactory signaling system in the kidney. *Proc. Natl. Acad. Sci. USA* **2009**, *106*, 2059–2064. [[CrossRef](#)] [[PubMed](#)]
21. Griffin, C.A.; Kafadar, K.A.; Pavlath, G.K. MOR23 promotes muscle regeneration and regulates cell adhesion and migration. *Dev. Cell* **2009**, *17*, 649–661. [[CrossRef](#)] [[PubMed](#)]
22. Busse, D.; Kudella, P.; Gruning, N.M.; Gisselmann, G.; Stander, S.; Luger, T.; Jacobsen, F.; Seinstraber, L.; Paus, R.; Gkogkolou, P.; *et al.* A synthetic sandalwood odorant induces wound-healing process in human keratinocytes via the olfactory receptor OR2AT4. *J. Investig. Dermatol.* **2014**, *134*, 2823–2832. [[CrossRef](#)] [[PubMed](#)]
23. Kim, S.H.; Yoon, Y.C.; Lee, A.S.; Kang, N.; Koo, J.; Rhyu, M.R.; Park, J.H. Expression of human olfactory receptor 10J5 in heart aorta, coronary artery, and endothelial cells and its functional role in angiogenesis. *Biochem. Biophys. Res. Commun.* **2015**, *460*, 404–408. [[CrossRef](#)] [[PubMed](#)]



24. Williams, S.D.; Ford, D.A. Activation of myocardial cAMP-dependent protein kinase by lysoplasmethylcholine. *FEBS Lett.* **1997**, *420*, 33–38. [[CrossRef](#)]

**Sample Availability:** Samples of the compounds are available from the authors.



© 2015 by the authors; licensee MDPI, Basel, Switzerland. This article is an open access article distributed under the terms and conditions of the Creative Commons by Attribution (CC-BY) license (<http://creativecommons.org/licenses/by/4.0/>).